NACA

# RESEARCH MEMORANDUM

## AN EXPERIMENTAL INVESTIGATION OF THE UNSTEADY LIFT INDUCED ON A WING IN THE DOWNWASH FIELD OF AN OSCILLATING CANARD CONTROL SURFACE

By David E. Reese, Jr.

Ames Aeronautical Laboratory
Moffett Field, Calif.





NATIONAL ADVISORY COMMITTEE
FOR AERONAUTICS

WASHINGTON
August 15, 1955

NATIONAL ADVISORY COMMITTEE FOR AERONAUTICS

RESEARCH MEMORANDUM

# AN EXPERIMENTAL INVESTIGATION OF THE UNSTEADY LIFT INDUCED ON A WING IN THE DOWNWASH FIELD OF AN OSCILLATING CANARD CONTROL SURFACE

By David E. Reese, Jr.

## SUMMARY

The results of an experimental investigation of the unsteady lift induced on a wing in the downwash field of an oscillating canard control surface are presented. The in-phase and out-of-phase components of the lift and their respective centers of pressure were measured at frequencies from 10 to 110 cycles per second over a Mach number range of 0.6 to 0.8 and 1.4 to 1.9 at angles of attack of $0^\circ$, $5^\circ$, and $10^\circ$.

The results indicated that existing theories provide a reliable guide for the estimation of the magnitude of the lift derivatives and centers of pressure at low values of reduced frequency and low angles of attack. An estimation of the effect of frequency on the lift derivatives was developed using a simple indicial function for the wing based on the lag-in-downwash concept. The trends of the data with frequency predicted by the theory were, in general, borne out by experiment at low angles of attack.

## INTRODUCTION

With the present trend in airframe configurations for guided missiles toward low-aspect-ratio wings and tails, the contribution of wing-tail interference effects to the over-all stability of the configuration has become of major importance. An accurate appraisal of these interference forces is necessary not only for the usual stability calculations but also in the design of automatic control equipment.

In an analysis of the response of a missile to various guidance commands, both static and dynamic forces and moments acting on the missile must be considered. The requirement of rapid response to these commands has focused increased attention on the dynamic quantities involved in the

calculations. One particular problem for canard-type missiles that has brought to light the need for information on dynamic interference forces is associated with the longitudinal dynamic stability of these missiles. In order to provide sufficient damping of the longitudinal motion of the missile, damping is often supplied artificially by actuating the forward control surfaces in proportion to the pitching velocity of the airframe. Since it is possible for a large portion of the total moment created in this manner to arise from the interference lift on the rear surfaces, it is necessary to know these dynamic interference effects with reasonable accuracy in order to predict the response of the missile. A knowledge of not only the magnitude of the interference lift but also its dependency on frequency is required.

Some theoretical estimates of static wing-tail interference forces have been made by Nielson, Kaattari, and Anastasio (ref. 1) and Schindel and Durgin (ref. 2). An experimental investigation of these forces and moments for several wing-tail combinations is presented in reference 3 by Schindel and Durgin. Some theoretical values for the time-dependent forces are given by Miles (ref. 4) and Martin, Dieterich, and Bobbitt (ref. 5) for very low frequencies. However, no published data on the experimental determination of these unsteady interference forces and moments are known to be available. The present experiment was, therefore, planned to meet this need.

## SYMBOLS

$C_{L_\delta}$ lift derivative in phase with control-surface position, positive upward, $\frac{57.3L_{IP}}{\frac{1}{2}\rho V^2 S\delta_o}$, per radian

$C_{L_{\dot{\delta}}}$ lift derivative out of phase with control surface position (in phase with control surface velocity), positive upward $\frac{57.3L_{OP}}{\frac{1}{2}\rho V^2 S\left(\frac{\dot{\delta}_o c}{2V}\right)}$, per radian

$L_{IP}$ lift in phase with control position, lb

$L_{OP}$ lift out of phase with control position, lb

M Mach number, $\frac{V}{\text{speed of sound}}$, dimensionless

S total area of wing, sq ft

| | |
|---|---|
| $V$ | free-stream speed, ft/sec |
| $c$ | wing chord, ft |
| $f$ | frequency of oscillation |
| $k$ | reduced frequency, $\frac{\omega l}{2V}$, dimensionless |
| $k_r$ | reduced frequency at wind-tunnel resonance, dimensionless |
| $l$ | distance from control surface centroid to wing centroid, ft |
| $q$ | dynamic pressure, $\frac{1}{2}\rho V^2$, lb/sq ft |
| $t$ | time, sec |
| $\left(\frac{\bar{x}}{c}\right)_{C_{L_\delta}}$ | center of pressure of in-phase lift, positive behind wing leading edge, dimensionless |
| $\left(\frac{\bar{x}}{c}\right)_{C_{L_{\dot{\delta}}}}$ | center of pressure of out-of-phase lift, positive behind wing leading edge, dimensionless |
| $\alpha$ | angle of attack of wing and body, deg |
| $\delta$ | instantaneous control-surface deflection, deg |
| $\dot{\delta}$ | instantaneous control-surface angular velocity, deg/sec |
| $\delta_o$ | maximum control-surface deflection, deg |
| $\dot{\delta}_o$ | maximum control-surface angular velocity, $\omega\delta_o$, deg/sec |
| $\rho$ | mass density of air, slugs/cu ft |
| $\varphi$ | phase angle between lift and angular position of control surface, deg |
| $\omega$ | angular frequency, $2\pi f$, radians/sec |

## THEORY

The purpose of this investigation is to determine the unsteady lift induced on a wing in the downwash field of an oscillating canard control surface. In this section, methods will be presented from which results can be obtained for the theoretical values of this lift. Frequency

effects on the phase relationship between the induced lift and the control deflection are of primary interest. For purposes of computation, the induced lift at frequencies near zero will be treated first, however, and then the effects of frequency will be studied. As is usually done in dynamic stability calculations, the amplitude of the unsteady lift will be divided into two components, one in phase with the control surface position and the other in phase with control surface velocity, the latter being commonly known as the out-of-phase lift. The model used for the theoretical analysis consisted of a canard control surface and a wing alone, that is, a bodyless model. The degree to which the body effects are considered in this report will be mentioned in a later section.

## Frequencies Near Zero

The amplitude of the in-phase lift derivative $C_{L_\delta}$ and its center of pressure at values of $k$ approaching zero were calculated by the method presented in reference 1. Since this procedure is commonly used in the calculation of the static lift and center of pressure of wing-body-tail combinations, it need not be discussed further here.

The calculations for the amplitude and center of pressure of the out-of-phase lift derivative $C_{L_{\dot{\delta}}}$ were based on the lag-in-downwash concept appearing in reference 6. In this approximation the assumption is made that the downwash at the rear surface will be that created by the forward surface at a small time $l/V$ earlier, where $l$ is taken to be the distance from the centroid of area of the control surface to the centroid of area of the wing. Thus

$$\Delta\epsilon_w = -\frac{d\epsilon_c}{d\delta}\frac{d\delta}{dt}\Delta t \tag{1}$$

where

$\Delta\epsilon_w$ change in downwash at the wing

$d\epsilon_c$ change in downwash at the control

then

$$\Delta\epsilon_w = -\frac{d\epsilon_c}{d\delta}\dot{\delta}\frac{l}{V} \tag{2}$$

The lift on the wing due to this change in downwash can be written

$$L_{OP} = - qS\Delta\epsilon_w(C_{L_\alpha})_w$$

$$= qS\dot{\delta}\,\frac{l}{V}\frac{d\epsilon_c}{d\delta}(C_{L_\alpha})_w \qquad (3)$$

Where $(C_{L_\alpha})_w$ is the lift-curve slope of the wing alone in uniform flow. But $d\epsilon_c(C_{L_\alpha})_w$ is the negative lift on the wing due to a small change in downwash $d\epsilon_c$. This negative lift divided by $d\delta$ is then $- C_{L_{\dot{\delta}}}$, so

$$L_{OP} = - qS\dot{\delta}\,\frac{l}{V}\,C_{L_{\dot{\delta}}} \qquad (4)$$

In coefficient form this lift is

$$C_{L_{\dot{\delta}}} = - 2\,\frac{l}{c}\,C_{L_{\dot{\delta}}} \qquad (5)$$

which corresponds to the answer obtained by Martin, Dieterich, and Bobbitt in reference 5.

## Frequency Effects

The effects of frequency on the lift derivatives at a Mach number of 1.7 were calculated using the response of the wing to an impulsive deflection of the control surface. This indicial response of the wing was calculated by methods presented by Tobak in reference 7. The indicial response was then converted to frequency response through the use of the Duhamel integral.

Since the calculations necessary to define the indicial lift response for the present problem were quite lengthy, they were carried out only for a Mach number of 1.7 and an angle of attack of $0^\circ$. However, it was found for this case that a good approximation to the frequency response obtained by the more exact solution could be made by assuming an indicial lift response based on the lag-in-downwash concept. This is an extension then, to include the effects of frequency, of the theory on which the low-frequency values of the out-of-phase lift derivative were based as given in the preceding section. In this approximation it is assumed that the wing experiences no lift until the downwash impulse from the control surface has reached the midchord of the wing. At that time the lift of the wing immediately assumes its steady-state value. This results in an indicial function of the form shown in sketch (a), where $t^*$ is

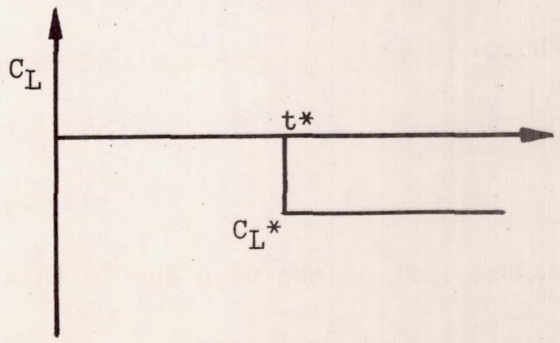


Sketch (a)

the time required for the pulse to travel from control surface midchord to wing midchord and $C_L^*$ is the steady-state value of the lift of the wing in the presence of the downwash from the control.

The time $t^*$ has an important physical meaning as is shown in reference 7. In that paper it is shown that the indicial lift of the wing due to the downwash from the suddenly deflected control surface has the form shown in sketch (b). It is also shown that, with the fulfillment of certain mild conditions, the time at which the indicial curve crosses the zero lift axis is very nearly equal to the time $t^*$ defined above. It was also found that, in frequency-response calculations of the derivatives $C_{L_\delta}$ and $C_{L_{\dot{\delta}}}$, the effects of the two shaded peaks tended, in large part, to cancel. Thus good correspondence between the results based on the simplified indicial response and those based on the more exact solution is indicated.

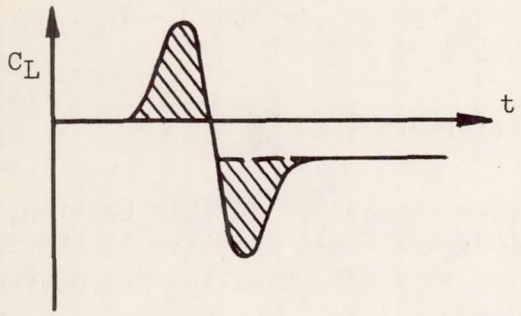


Sketch (b)

Once the indicial function has been defined, it is possible to obtain the variation of the lift on the wing with frequency through the use of the Duhamel integral. In reference 7 Tobak has used the Duhamel integral to derive the following equations for the in-phase and out-of-phase lift derivatives in terms of the indicial functions of the wing:

$$C_{L_\delta} = C_{L_\delta}^* - k'\int_0^\infty F_1(\theta)\sin k'\theta \, d\theta + k'^2\int_0^\infty F_2(\theta)\cos k'\theta \, d\theta \qquad (6)$$

$$C_{L_{\dot{\delta}}} = C_{L_q}^* - \int_0^\infty F_1(\theta)\cos k'\theta \, d\theta - k'\int_0^\infty F_2(\theta)\sin k'\theta \, d\theta \qquad (7)$$

where

$$F_1(\theta) = C_{L_\delta}(\theta) - C_{L_\delta}^*$$

$$F_2(\theta) = C_{L_q}(\theta) - C_{L_q}^*$$

and

$C_{L_\delta}(\theta)$ indicial response of the wing to a step deflection $\delta$ of the control surface

$C_{L_\delta}$* steady-state lift on the wing due to a deflection $\delta$ of the control surface

$C_{L_q}(\theta)$ indicial response of the wing to a step change in pitching velocity q of the control surface

$C_{L_q}$* steady-state lift on the wing due to a pitching velocity q of the control surface

$\theta$ nondimensional time parameter = $\frac{2Vt}{c}$

k' reduced frequency, defined in reference 7 as $\frac{\omega c}{2V}$

It can be shown that, for the problem considered in this section, $C_{L_q}$* and the integrals containing $F_2(\theta)$ are small relative to the remaining terms in the equations. Making this approximation and noting that $k' = \frac{c}{l} k$, we reduce equations (6) and (7) to

$$C_{L_\delta} = C_{L_\delta}{}^* - \frac{c}{l} k \int_0^\infty F_1(\theta) \sin \frac{c}{l} k\theta \, d\theta \tag{8}$$

$$C_{L_{\dot\delta}} = - \int_0^\infty F_1(\theta) \cos \frac{c}{l} k\theta \, d\theta \tag{9}$$

Performing the integrations indicated in equations (8) and (9) on the indicial function defined in sketch (a), we derive the following relationships:

$$C_{L_\delta} = C_{L_\delta}{}^* \cos 2k \tag{10}$$

$$C_{L_{\dot\delta}} = - \frac{l}{c} C_{L_\delta}{}^* \frac{\sin 2k}{k} \tag{11}$$

These expressions give the values of the in-phase and out-of-phase lift derivatives as functions of frequency. It is apparent that the limiting values of equations (10) and (11) as k approaches zero give the results obtained in the preceding section.

The phase angle between the induced lift and the control deflection is

$$\varphi = \tan^{-1} \frac{L_{OP}}{L_{IP}} = \tan^{-1} \frac{(\omega c/2V) C_{L_{\dot\delta}}}{C_{L_\delta}} \tag{12}$$

Substituting the expressions from (10) and (11) in equation (12), we find that

$$\varphi = \pi - 2k \text{ radians} \tag{13}$$

In order to obtain the variation of the centers of pressure of the in-phase and out-of-phase lifts with frequency it was necessary to obtain values for the in-phase and out-of-phase pitching moments corresponding to those found for the lift in equations (10) and (11). For this problem the indicial variation of the pitching moment with time was again that shown in sketch (a). While the calculations are not shown, it is apparent that the expressions for the pitching moments will be identical to equations (10) and (11) with the substitution of the appropriate moment derivatives for the lift derivatives. Since center of pressure is defined as pitching moment divided by lift, it can be seen that both the centers of pressure of the in-phase and out-of-phase lifts are equal to the center of pressure for the steady-state case and that there is no variation of center of pressure with frequency. Therefore the method of reference 1 was used to calculate these values.

## APPARATUS

### Wind Tunnel

The investigation was conducted in the Ames 6- by 6-foot supersonic wind tunnel which is of the closed-return, variable-density type and which has a Mach number range of 0.6 to 0.9 and 1.2 to 1.9. A detailed description of the flow characteristics of this wind tunnel can be found in reference 8.

### Model

The model consisted of a rectangular wing and a rectangular control surface mounted in canard arrangement on a slender cylindrical body of fineness ratio 14. The dimensions of the model are given in figure 1. Both the wing and the control surface were composed of 5-percent-biconvex, circular-arc airfoil sections. A 5-inch, hollow, circular cylinder fitted with an ogival nose served as the body. The model was fabricated from steel with the exception of the nose and wing. The nose section was made of fiberglass-reinforced plastic while the wing was made from magnesium to reduce its mass to a minimum. A three-phase induction motor was used to rotate the control surface in near sinusoidal oscillations about its midchord by means of the drive linkage shown in figure 2. The model was sting mounted in the wind tunnel and a strut was used to stiffen the body against the oscillating loads produced by the control surface. The location and dimensions of the strut are given in figure 1.

## TECHNIQUE AND INSTRUMENTATION

There were four quantities obtained during this investigation: the amplitude of the oscillating lift induced on the wing in phase with the angular position of the control surface, the amplitude of the oscillating lift induced on the wing in phase with the angular velocity of the control surface, and their respective centers of pressure. The measurement of unsteady forces such as those encountered in this investigation usually necessitates equipment in the nature of an oscillograph or an oscilloscope to record or view the dynamic signals. The use of such equipment is somewhat inconvenient compared with that utilized in static tests in that, in many cases, the desired quantities are not indicated directly and additional steps such as film reading and harmonic analysis must be added to the data-reduction process before the final result is obtained. It would be desirable, then, to use a technique that would eliminate these additional steps and make it possible to read the peak magnitudes of the dynamic quantities directly.

The technique and instrumentation employed in this investigation permitted the rapid, direct measurement of the peak magnitudes of the in-phase and out-of-phase components of the lift on the wing. The method consisted of multiplying a signal proportional to the induced lift on the wing by a sine or cosine signal in phase with the control-surface position and velocity, respectively. These two products can be written as:

$$P_{sin} = \sin \omega t \; L_1 \sin(\omega t + \varphi) \tag{14}$$

$$P_{cos} = \cos \omega t \; L_1 \sin(\omega t + \varphi) \tag{15}$$

where

$L_1 \sin(\omega t + \varphi)$ the oscillating lift induced on the wing

$\varphi$ phase angle between the oscillating lift and the angular position of the control surface

$P_{sin}$ product of the sine signal and the oscillating lift

$P_{cos}$ product of the cosine signal and the oscillating lift

Equations (14) and (15) can be rewritten as:

$$P_{sin} = \frac{L_1}{2} [\cos \varphi - \cos(2\omega t + \varphi)] \tag{16}$$

$$P_{cos} = \frac{L_1}{2} [\sin \varphi + \sin(2\omega t + \varphi)] \tag{17}$$

But the magnitude of the in-phase lift is defined as $L_1 \cos \varphi$ and that of the out-of-phase lift is defined as $L_1 \sin \varphi$. Thus, it is evident that if the time-varying portions of the product signals are filtered out, the remaining parts are proportional to the components of the lift in phase with the angular position and angular velocity of the control surface.

The technique described above can be realized with a system made up of three parts: a load measuring device capable of producing a signal proportional to the induced lift of the wing, a circuit producing the sine and cosine signals, and an indicating device that will respond only to steady signals. The force induced on the exposed portion of the wing was indicated by strain gages mounted on the wing supports. The arrangement of these strain-gage members is shown in figure 3. In all, eight strain-gage bridges were used, two on each of the four wing supports. In order to compensate for any spanwise movement of the center of pressure, each bridge on the left side of the body center line was connected in parallel with its counterpart on the right side. Thus there were four bridge pairs, two located at the wing leading edge and two located at the trailing edge. This arrangement of strain-gage circuits provided duplicate indication of the components of the induced lift acting at the leading and trailing edges of the wing, and the dual circuits were then used to find the in-phase and out-of-phase parts of these lifts. The sum of the in-phase lifts at the leading and trailing edges gave the total in-phase lift while the ratio of the lift at the trailing edge to the total lift gave the distance of the center of pressure from the leading edge in percent chord. These calculations were also carried out for the out-of-phase lift.

The product of the force signal with a sine or cosine signal was obtained by using a sine or cosine voltage as power for the strain-gage circuits. The output of the gage circuit was then proportional to the stress in the gage multiplied by the applied voltage signal. The sine and cosine voltages were produced by a circuit which utilized a commercial induction resolver whose armature was driven by the motor driving the control surface. A 20-kc sinusoidal carrier wave was used as an input signal to the resolver. This carrier wave was modulated sinusoidally by the resolver at the drive frequency to give two output signals with a $90^\circ$ phase difference. These signals were each passed through a half-wave rectifier and filter to remove the carrier frequency and amplified to the level needed to drive the strain-gage circuit.

The outputs of the strain-gage circuits were connected to light-beam galvanometers. The frequency response of these galvanometers can be described adequately by the response of a spring-mass-damper system. The differential equation of motion for the system is:

$$m\ddot{x} + c\dot{x} + kx = P \sin \omega t \qquad (18)$$

and the solution to this equation is

$$x = \frac{x_{st}}{\sqrt{\left[1 - \left(\frac{\omega}{\omega_o}\right)^2\right]^2 + 4\zeta^2\left(\frac{\omega}{\omega_o}\right)^2}} \sin(\omega t + \epsilon) \qquad (19)$$

where

$$\epsilon = \tan^{-1} \frac{2\zeta \frac{\omega}{\omega_o}}{1 - \left(\frac{\omega}{\omega_o}\right)^2}$$

and

$x_{st}$ static deflection of the galvanometer to a steady signal of magnitude P.

$\omega_o$ natural frequency of galvanometer, $\sqrt{\frac{k}{m}}$

$\zeta$ damping ratio of galvanometer, $\frac{c}{2\sqrt{km}}$

Examination of equation (19) shows that if the ratio of the signal frequency $\omega$ to the natural frequency $\omega_o$ is sufficiently large, the response of the galvanometer to the signal is essentially zero. The response is also decreased by a high damping ratio. The galvanometers used during this investigation had sufficiently low natural frequencies and high damping that no response was observed to signals of 10 cycles per second or greater. As a result, the galvanometers acted as filters to remove the time-varying portions of the strain-gage signals and only the steady part of the signal was indicated.

## TESTS

The investigation of the unsteady lift induced on the wing by an oscillating canard control surface was conducted over a Mach number range of 0.6 to 0.8 and 1.4 to 1.9 at angles of attack of $0^\circ$, $5^\circ$, and $10^\circ$. The minimum supersonic Mach number was chosen such that the reflection from the tunnel walls of the shock waves from the control surface fell behind the wing trailing edge. A constant Reynolds number of $1.67 \times 10^6$ based on wing chord was held for the entire test.

The control surface was driven at frequencies from 10 to 110 cycles per second covering reduced-frequency ranges of 0.06 to 0.70 at a Mach number of 1.9 and 0.15 to 1.80 at a Mach number of 0.6. The maximum amplitude of the control surface oscillations was fixed by the drive linkage at $5^\circ$.

## CORRECTIONS TO DATA

The only corrections made to the data obtained in the subsonic speed range were to the Mach number and dynamic pressure of the flow. It was recognized that the phenomenon of wind-tunnel resonance and its effect on the air forces acting on an oscillating two-dimensional wing has been predicted on a theoretical basis and that experimental verification of this theory has been made (ref. 9). However, the author knows of no published corrections for the effects of tunnel walls on the oscillatory air forces of a subsonic three-dimensional wing. Woolston and Runyan in reference 10 give an equation for the resonant frequency of a tunnel having a rectangular cross section which has been used to calculate tunnel resonant frequencies for this investigation. These frequencies are shown in their appropriate places with the data and will be discussed more fully in a subsequent section.

The Mach number and dynamic pressure of the subsonic flow were corrected for blockage effects by the method presented in reference 11. At a Mach number of 0.8, these corrections amounted to an increase of about 1.5 percent in the Mach number and dynamic pressure over the value obtained from measurements made without a model in the tunnel.

No corrections were made to either the flow conditions or the lift data at supersonic speeds.

The possibility of errors due to air-stream fluctuations of a periodic nature was considered. These periodic fluctuations could be caused by tunnel turbulence, an oscillating wake shed from the nose of the model at angle of attack, or possibly by the wake from the supporting strut. In order to evaluate this effect, a series of tests were made on the model with the control surface removed. These tests showed that there were no periodic fluctuations in the air stream of measurable magnitude for the range of Mach numbers, frequencies, and angles of attack covered in this investigation.

## PRECISION OF DATA

In the section "Technique and Instrumentation," the system used in this investigation was presented in its simplest form in order to show the essential features of its operation. As could be expected, actual practice proved the system to be more complex than was indicated from simple considerations. These complexities, as it turned out, determined the accuracy of the final results. In this section, the various factors that contributed to a departure from the elementary system mentioned previously will be discussed in terms of their relationship to the precision of the data.

The usual starting point for a discussion of the precision of the data is concerned with the least readings of the quantities involved in the reduction of the data to coefficient form. For this investigation these readings were as follows: lift, 0.05 pound; stagnation temperature, 2° Fahrenheit; stagnation pressure, 0.2 centimeter of mercury; period of oscillation (1/f), 0.0001 second. The total uncertainty in the coefficients due to least readings was taken as the square root of the sum of the squares of the effects of these least readings. This calculation led to uncertainties of ±0.003 for $C_{L_\delta}$, ±0.12 for $C_{L_{\dot{\delta}}}$, ±0.005 for center of pressure, and ±0.5° for $\varphi$.[1]

In the earlier description of the technique, the expressions for the terms in the product signals (eqs. (14) and (15)) were written in an idealized form. In general, however, the strain-gage output cannot be expressed as a simple sine function but will also contain a steady term and harmonics of the fundamental frequency. These harmonics could arise from the distortion in the control-surface motion produced by the drive mechanism or from a nonlinear response of the downwash to the control deflection. The driving voltages could also contain harmonics introduced by the electronic circuitry producing them. Therefore, the signals must be written as:

$$L = L_0 + \sum_{n=1}^{\infty} L_n \sin(n\omega t + \varphi_n) \tag{20}$$

$$v_{sin} = \sum_{n=1}^{\infty} B_m \sin(m\omega t + \theta_m) \tag{21}$$

$$v_{cos} = \sum_{m=1}^{\infty} C_m \cos(m\omega t + \epsilon_m)$$

where

L total lift on the wing

$v_{sin}$ sine voltage

$v_{cos}$ cosine voltage

[1]It should be noted that the uncertainty due to least reading becomes very large as the lift forces approach zero. The values given here are for average values of in-phase and out-of-phase lift.

$L_o$ steady lift on the wing

$L_n$ amplitude of the nth harmonic of the oscillating lift

$\varphi_n$ phase angle between the nth harmonic of the lift and the position of the control surface

$B_m$ amplitude of the mth harmonic of the sine voltage

$\theta_m$ phase angle between the mth harmonic of the sine voltage and the position of the control surface

$C_m$ amplitude of the mth harmonic of the cosine voltage

$\epsilon_m$ phase angle between the mth harmonic of the cosine voltage and the velocity of the control surface

The products of the lift and the sine or cosine signal are then

$$P_{sin} = L_o \sum_{m=1}^{\infty} B_m \sin(m\omega t + \theta_m) + \sum_{n=1}^{\infty} \sum_{m=1}^{\infty} L_n B_m \sin(n\omega t + \varphi_n) \sin(m\omega t + \theta_m)$$

$$= L_o \sum_{m=1}^{\infty} B_m \sin(m\omega t + \theta_m) + \sum_{n=1}^{\infty} \sum_{m=1}^{\infty} \frac{L_n B_m}{2} \left\{ \cos[(n - m)\omega t + \varphi_n - \theta_m] - \right.$$

$$\left. \cos[(n + m)\omega t + \varphi_n + \theta_m] \right\} \tag{22}$$

$$P_{cos} = L_o \sum_{m=1}^{\infty} C_m \cos(m\omega t + \epsilon_m) + \sum_{n=1}^{\infty} \sum_{m=1}^{\infty} L_n C_m \sin(n\omega t + \varphi_n) \cos(m\omega t + \epsilon_m)$$

$$= L_o \sum_{m=1}^{\infty} C_m \cos(m\omega t + \epsilon_m) + \sum_{n=1}^{\infty} \sum_{m=1}^{\infty} \frac{L_n C_m}{2} \left\{ \sin[(n - m)\omega t + \varphi_n - \epsilon_m] + \right.$$

$$\left. \sin[(n + m)\omega t + \varphi_n + \epsilon_m] \right\} \tag{23}$$

Examination of equations (22) and (23) shows that the only terms in the expressions that are not functions of time arise from the products of like harmonics in the lift signal and driving voltage. Thus the signals indicated by the galvanometers are:

$$P_{sin} = \frac{L_1 B_1}{2} \cos(\varphi_1 - \theta_1) + \frac{L_2 B_2}{2} \cos(\varphi_2 - \theta_2) + \ldots \quad (24)$$

$$P_{cos} = \frac{L_1 C_1}{2} \sin(\varphi_1 - \epsilon_1) + \frac{L_2 C_2}{2} \sin(\varphi_2 - \epsilon_2) + \ldots \quad (25)$$

The desired quantities are, of course, the in-phase and out-of-phase components of the fundamental amplitude of the lift, that is, $L_1 \cos \varphi_1$ and $L_1 \sin \varphi_1$.

It can be seen then that the higher harmonics can produce spurious signals which would lead to erroneous results.

Since no measurements were made of the harmonic content of the lift signal, it was not possible to determine quantitatively what errors were introduced from this source. However, harmonic analyses of the output of the resolver circuits were made during calibration and it was found that there was 7 percent of the fundamental amplitude present as second harmonic and 1 percent as third harmonic in both the sine and cosine voltages for the frequency range of the investigation. All higher harmonics were negligible. Thus if $B_1 = 1$, then $B_2 = 0.07$, $B_3 = 0.01$ and $B_4, B_5, \ldots = 0$. Hence, if the amplitude of the second harmonic equals that of the fundamental in the lift signal, the error in the measurement of the fundamental amplitude would be 7 percent. It can be seen therefore that the low harmonic content of the sine and cosine voltages reduces any error due to harmonic content of the lift force.

The misalinement of the resolver was another factor that could lead to error in the final result. This misalinement can be thought of in terms of a phase angle between the sine and cosine voltages and the position and velocity of the control surface, respectively. The resolver would be perfectly alined if these phase angles were zero. The general form of the products written above incorporated these phase angles. Inasmuch as it has been shown that the effects of the second harmonics, or higher, are small, only the alinement of the fundamental amplitude of the resolver signals was considered. Calibrations were made during the course of testing which showed that the average values of $\theta_1$ and $\epsilon_1$ were about $0.5^\circ$ each. It can be shown that a resolver misalinement of $0.5^\circ$ will introduce an error of not more than $0.5^\circ$ in the calculation of the phase angle $\varphi_1$.

The remaining factor to be discussed with regard to the precision of the data is the response of the mechanical system to oscillating loads.

It was recognized that the output of the strain gages indicating the lift on the wing would be influenced by the response of the various parts of the mechanical system to the oscillating loads. In order to obtain a quantitative measure of this influence, a series of calibrations were made on the model in place in the wind tunnel by applying an oscillating force of known magnitude and measuring the amplitude and phase response of the system indicated by the output of the strain gages as the frequency of the input force was varied. These calibrations showed that above a frequency of 110 cycles per second, the natural frequency of the wing panels in bending (140 cps) introduced large errors in both amplitude and phase angle. In addition, it was found that the body natural frequency in bending occurred at approximately 85 cycles per second. However, the influence of this resonant peak on the response of the system was restricted to a narrow frequency band. Thus, by testing over a frequency range up to 110 cps and omitting a band near 85 cps, large errors arising from resonance of parts of the mechanical system were eliminated. With these regions eliminated, the results of the calibrations still showed small deviations from the ideal response. Since this scatter was greater than any known inaccuracies in the instrumentation, it was felt that it should be attributed to the response of the mechanical system and therefore had to be taken into account in the precision of the results. The calibrations showed that the root-mean-square deviation of the indicated force from the true force was ±6.4 percent of the true force, the rms deviation of center of pressure was ±0.02 wing chord, and the rms deviation of the phase angle from zero was ±1.7°.

It can be seen that the scatter in the results of the frequency-response calibrations for the mechanical system is the primary factor in the determination of the precision of the final result. The calculation of the uncertainty in the results including the effects of least reading, resolver misalinement, and mechanical-response errors led to values ±0.024 for $C_{L_\delta}$, ±0.24 for $C_{L_{\dot{\delta}}}$, ±0.02 for $\bar{x}/c$, and ±1.9° for $\varphi$.

## RESULTS AND DISCUSSION

The results of the experimental investigation of the unsteady lift induced on a wing in the downwash field of an oscillating canard control surface are shown in figures 4 through 8 as a function of reduced frequency for several Mach numbers and angles of attack. The nondimensional lift derivatives in phase and out of phase with control-surface position are presented in figures 4 and 5, while their respective centers of pressure are shown in figures 6 and 7. The variation of phase angle with reduced frequency is shown in figure 8 for the data obtained at $\alpha = 0°$. It should be noted that, since the experimental values of the lift derivatives were obtained by dividing the lift by $\delta_o$ or $\dot{\delta}_o$, the assumption is implicit that lift is a linear function of $\delta$ and $\dot{\delta}$.

Also shown on these figures are the corresponding theoretical values computed using equations (10), (11), and (13). The values of static lift, $C_{L_\delta}$*, used in these calculations were computed by the method of reference 1. Thus, while the theoretical development of equations (10), (11), and (13) was based on a bodyless model, the calculated values of $C_{L_\delta}$* were based on wing-body theory. In other words, it has been assumed that the body affects the initial values of the lift derivatives ($k \rightarrow 0$) but does not affect their dependency upon frequency given in equations (10) and (11).

In-phase lift derivative.- Figure 4 is a plot of the in-phase lift derivative $C_{L_\delta}$ versus reduced frequency for the Mach numbers and angles of attack covered. Examination of this figure shows that the theory of reference 1 provides a reliable guide to the estimation of $C_{L_\delta}$ at low frequencies for an angle of attack $0^\circ$. In addition, the theoretical trends of $C_{L_\delta}$ with frequency calculated using the simplified indicial response were, in general, borne out by the experimental data for this angle of attack. At the higher angles of attack, however, there were some departures from the theory. For supersonic Mach numbers, the primary differences were in magnitude. The trend of the data with frequency remained the same as the angle of attack increased. At subsonic speeds, large variations in both magnitude and trend with frequency appeared. This was most noticeable at an angle of attack of $10^\circ$. While there is not sufficient evidence to explain this result conclusively, partial separation of the flow over the control surface may be one of the causes. Static tests of a similar wing (ref.12) show that at subsonic speeds, the flow begins to separate at an angle of attack of about $10^\circ$ and that the lift no longer increases with increasing angle of attack above $16^\circ$. Since the angle of attack of the control surface varied from $5^\circ$ to $15^\circ$ during each cycle when the body angle of attack was at $10^\circ$, the character of the flow was probably changing radically through each cycle, thereby affecting the lift induced on the wing.

The possibility of an effect of wind-tunnel resonance on the data obtained at subsonic speeds must be considered. The wind-tunnel resonant frequencies, $k_r$, are shown in the figures in terms of reduced frequency for each of the subsonic Mach numbers. It was shown in reference 9 that, for the two-dimensional case, the effect of tunnel resonance is to decrease the lift markedly near the resonant frequency. Examination of the data obtained in this investigation indicates that if a wind-tunnel resonance phenomenon exists for this particular combination of model and tunnel, it does not have the simple effect indicated in reference 9.

A comparison of the results calculated by the simplified indicial response and those calculated by the more exact indicial response is shown in figure 4(b) for a Mach number of 1.7. It is apparent that the differences are quite small over a large portion of the frequency range, thus corroborating the statement concerning this fact made in section "Theory."

It may be well to mention here the point brought out in the introduction concerning artificial damping for canard-type missiles. Since damping may be added by motion of the control surface proportional to the missile pitching velocity, the in-phase lift shown in figure 4 contributes to the damping of the missile. The results show that if the pitching frequency is sufficiently high, there would be a serious reduction and possibly a reversal of the damping moment supplied by the rear surface. However, the probability that the pitching frequency will reach these values appears small.

Out-of-phase lift derivative.- The lift derivative out of phase with control deflection, $C_{L_{\dot{\delta}}}$, is shown plotted versus reduced frequency in figure 5. Here the predictions of the theory are confirmed by the experiment for $\alpha = 0^\circ$ at subsonic speeds. However, as was the case for the in-phase derivative, the agreement between experiment and theory became poorer as the angle of attack increased, with the data obtained at $\alpha = 10^\circ$ showing a marked difference from that obtained at the lower angles.

In the supersonic speed range, the theoretical values of $C_{L_{\dot{\delta}}}$ at low frequencies show somewhat better agreement with experiment at $\alpha = 0^\circ$ than at the higher angles of attack. However, the decrease in $C_{L_{\dot{\delta}}}$ with increase in the frequency predicted by the simplified indicial response is not reflected in the experimental values. Examination of figure 5(b) shows that the more exact indicial-response result is similar to that for the simplified indicial response. Calculations of the values of $C_{L_{\dot{\delta}}}$ have shown that the frequency response of this derivative is highly sensitive to changes in the details of the indicial curve. Hence, better agreement could be achieved with a more refined indicial function.

Center of pressure of in-phase lift.- The experimental values of the center of pressure of the in-phase lift are shown in figure 6 along with the theoretical values for $\alpha = 0^\circ$. The theoretical values were calculated by the method of reference 1. Since this method is based on linear theory, no variations of center of pressure with angle of attack are predicted.

The theory of reference 1 predicts the location of the center of pressure very well for all Mach numbers at low frequencies and low angles of attack. In addition, the lack of variation with frequency predicted by the simplified indicial approach is borne out by the experimental data over most of the frequency range. The large deviations from the theoretical values were obtained either for conditions where the in-phase lift was near zero, thus affecting the accuracy of measurement, or at $\alpha = 10^\circ$ for subsonic Mach numbers where it is known that the lift forces themselves do not follow the predicted results.

Center of pressure of out-of-phase lift.- The experimental data for center of pressure of the out-of-phase lift, presented in figure 7,

confirms, in general, both the magnitude and trend with frequency predicted by the theory (excluding the data at $\alpha = 10^{\circ}$). At the lower frequencies, the data obtained in the subsonic speed range show values somewhat forward of those predicted by theory, but at supersonic speeds agreement is good throughout the frequency range.

Phase angle.- Perhaps the most direct application of the lag-in-downwash concept is to the calculation of the phase angle of the lift induced on the wing. Here, the time necessary for a disturbance to travel from the forward surface to the rear surface - the lag - can be converted directly to a phase angle for a given frequency. Figure 8 shows a comparison between this theory and the phase angles obtained at all Mach numbers for an angle of attack of $0^{\circ}$. It can be seen that this simple theory predicts the experimental variation of phase angle with frequency adequately for all Mach numbers for values of $k$ up to about 1.0. Beyond that value the experimental results are somewhat higher than theory. While only the phase angles for $\alpha = 0^{\circ}$ are presented in this figure, the phase angles for the other angles of attack, with the exception of those obtained at $\alpha = 10^{\circ}$ and subsonic speeds, showed the same variation with reduced frequency.

## CONCLUSIONS

An experimental investigation of the unsteady lift induced on a wing by the downwash field of an oscillating canard control surface led to the following conclusions:

1. Existing theories provided a reliable guide to the estimation of the magnitudes of the in-phase and out-of-phase lift derivatives and their respective centers of pressure at low values of reduced frequency and low angles of attack.

2. The trends of the data with frequency calculated with the use of a simple indicial lift response for the wing were, in general, confirmed by the experimental results at low angles of attack.

Ames Aeronautical Laboratory
National Advisory Committee for Aeronautics
Moffett Field, Calif., June 1, 1955

## REFERENCES

1. Nielson, Jack N., Kaattari, George E., and Anastasio, Robert F.: A Method for Calculating the Lift and Center of Pressure of Wing-Body-Tail Combinations at Subsonic, Transonic, and Supersonic Speeds. NACA RM A53G08, 1953.

2. Schindel, Leon H., and Durgin, Frank H.: Wing-Tail Interference at Supersonic Speeds. M.I.T. Naval Supersonic Lab., Tech. Rep. 8, 1953.

3. Schindel, Leon H., and Durgin, Frank H.: Forces on Tails in a Measured Supersonic Downwash Field. M.I.T. Naval Supersonic Lab., Wind Tunnel Rep. 33, Oct. 1952.

4. Miles, John W.: The Application of Unsteady Flow Theory to the Calculation of Dynamic Stability Derivatives. (Project MX-770) North American Aviation, Inc., Los Angeles. Aerophysics Lab. AL-957, Sept. 8, 1950.

5. Martin, John C., Dieterich, Margaret S., and Bobbitt, Percy J.: A Theoretical Investigation of the Aerodynamics of Wing-Tail Combinations Performing Time-Dependent Motions at Supersonic Speeds. NACA TN 3072, 1954.

6. Jones, B. Melvill: Dynamics of the Airplane. Symmetric or Pitching Motions. Vol V of Aerodynamic Theory, div. N, ch. II, sec. 40, W. F. Durand, ed., Julius Springer (Berlin), 1935, p. 50. (Available as CIT Reprint, 1944)

7. Tobak, Murray: On the Use of the Indicial Function Concept in the Analysis of Unsteady Motions of Wings and Wing-Tail Combinations. NACA Rep. 1188, 1954.

8. Frick, Charles W., and Olson, Robert N.: Flow Studies in the Asymmetric Adjustable Nozzle of the Ames 6- by 6-Foot Supersonic Wind Tunnel. NACA RM A9E24, 1949.

9. Runyan, Harry L., Woolston, Donald S., and Rainey, A. Gerald: A Theoretical and Experimental Study of Wind-Tunnel-Wall Effects on Oscillating Air Forces for Two-Dimensional Subsonic Compressible Flow. NACA RM L52I17a, 1953.

10. Woolston, Donald S., and Runyan, Harry L.: Some Considerations on the Air Forces on a Wing Oscillating Between Two Walls for Subsonic Compressible Flow. IAS Preprint 446, 1954.

11. Herriot, John G.: Blockage Corrections for Three-Dimensional-Flow Closed-Throat Wind Tunnels with Consideration of the Effect of Compressibility. NACA Rep. 995, 1950. (Formerly NACA RM A7B28)

12. Nelson, Warren A., and Frank, Joseph L.: The Effect of Wing Profile on the Transonic Characteristics of Rectangular and Triangular Wings Having an Aspect Ratio of 3 - Transonic Bump Technique. NACA RM A54H12a, 1954.

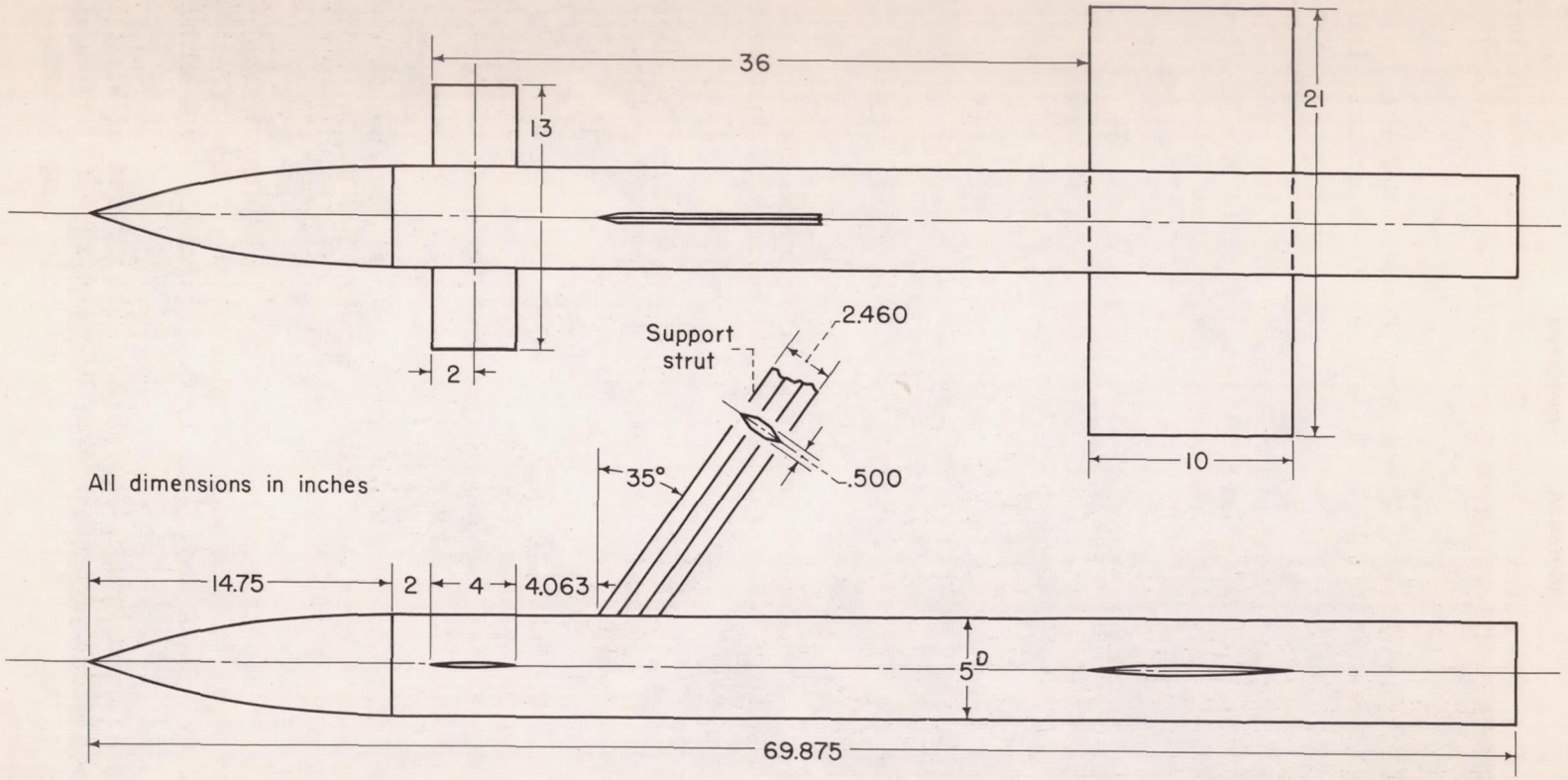


Figure 1.- Sketch of model.

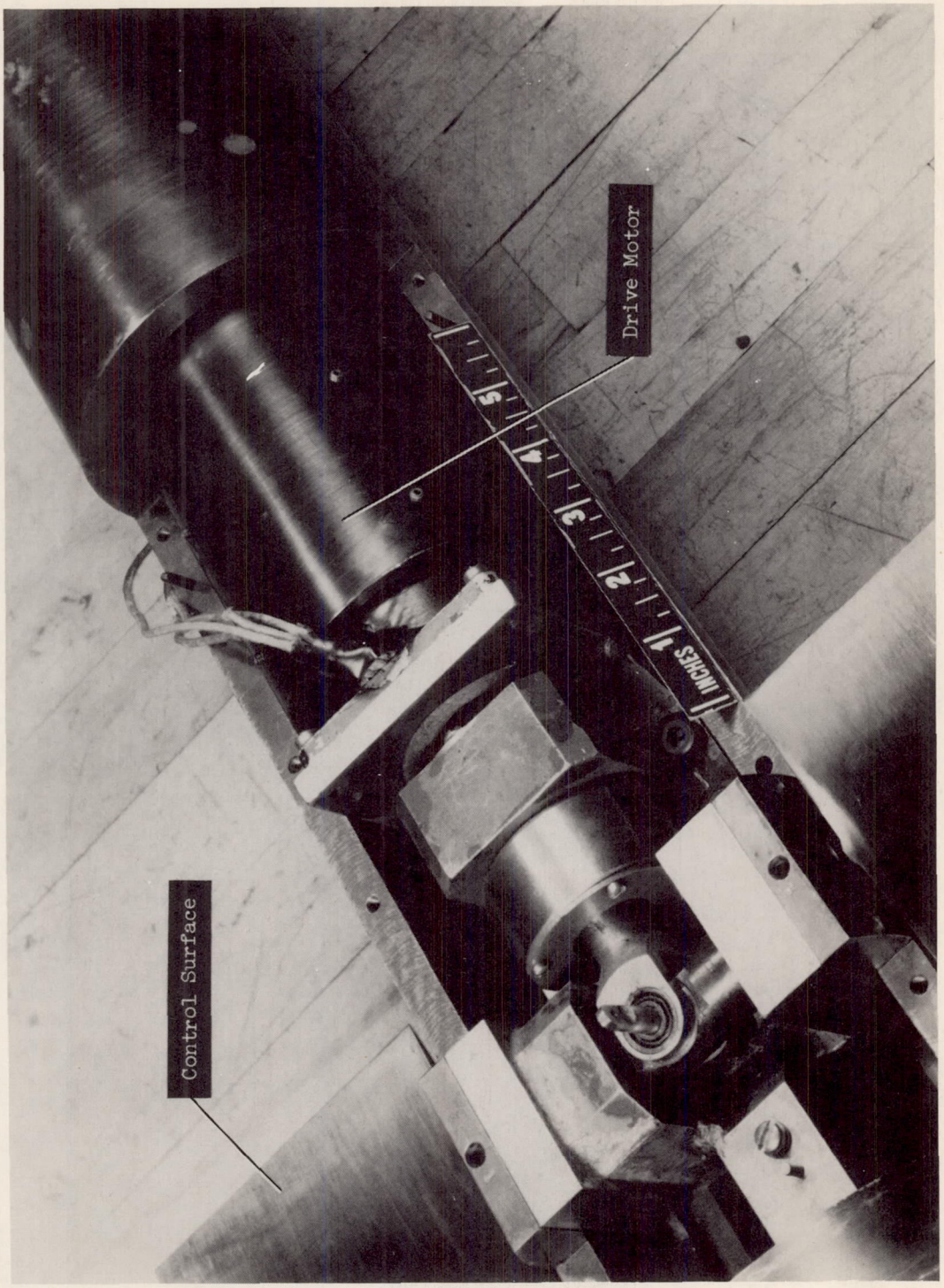


Figure 2.- Photograph of drive system.

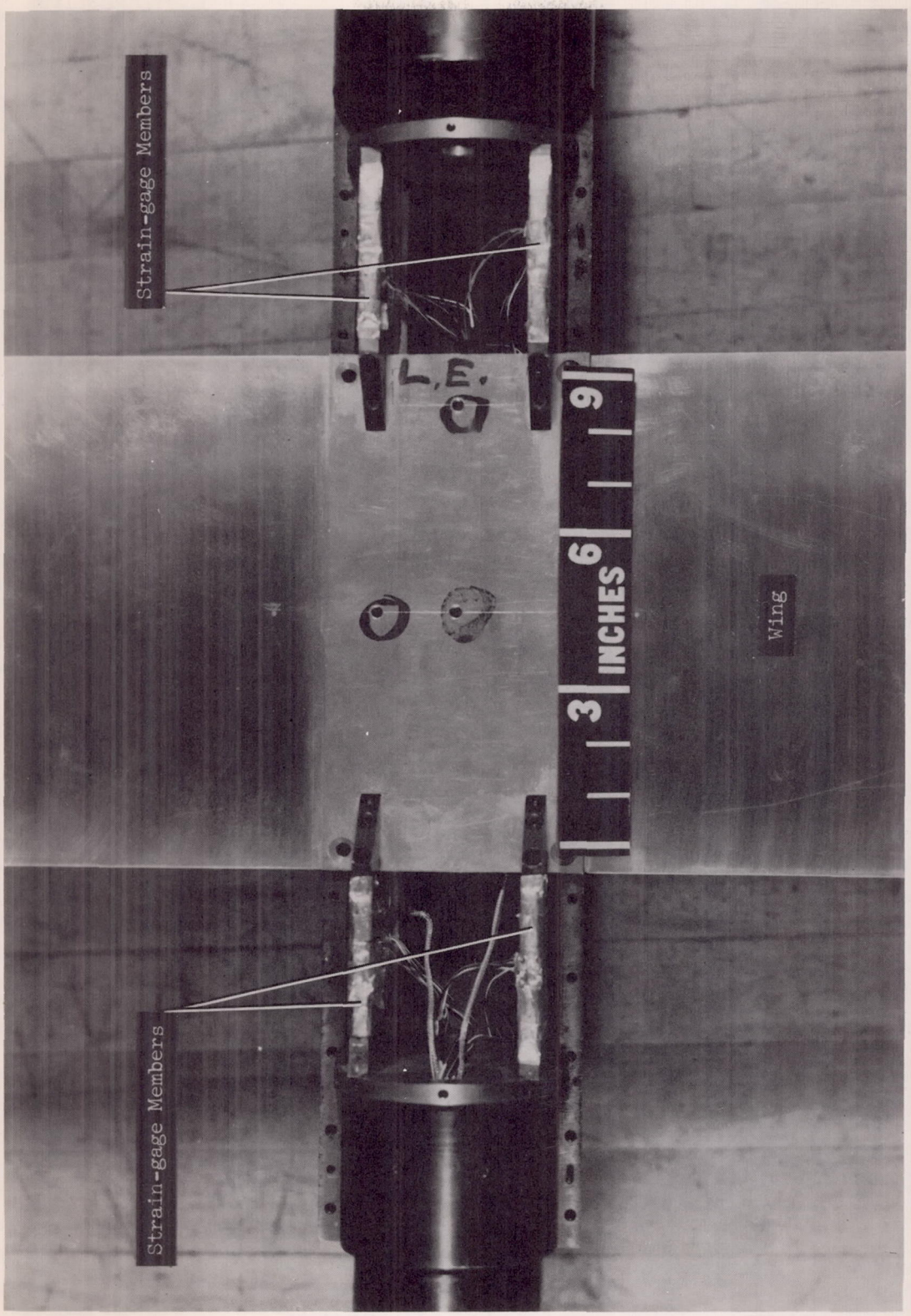


A-19493.1

Figure 3.- View of wing and strain-gage members.

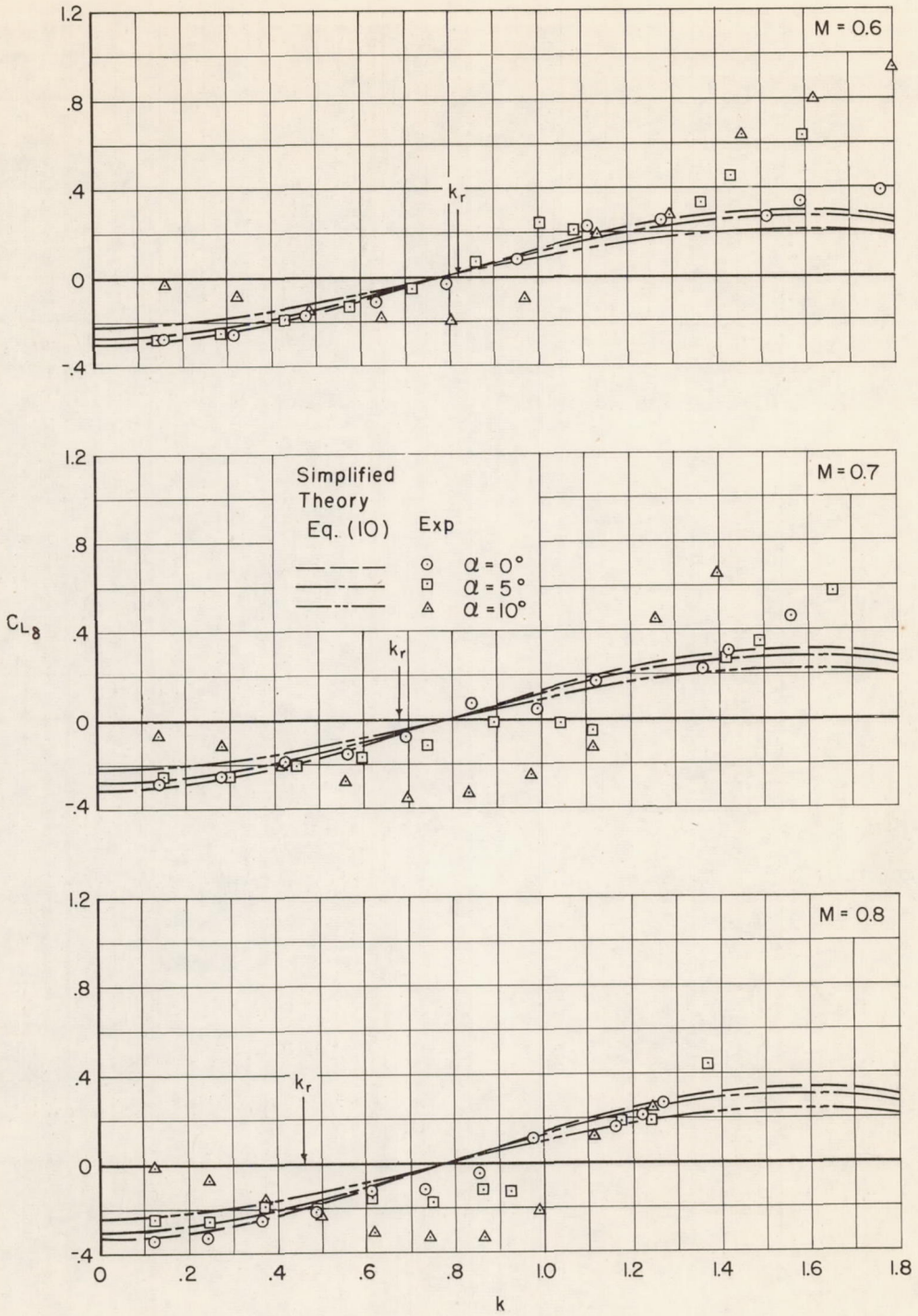


(a) Subsonic Mach numbers.

Figure 4.- Variation of in-phase lift derivative with reduced frequency.

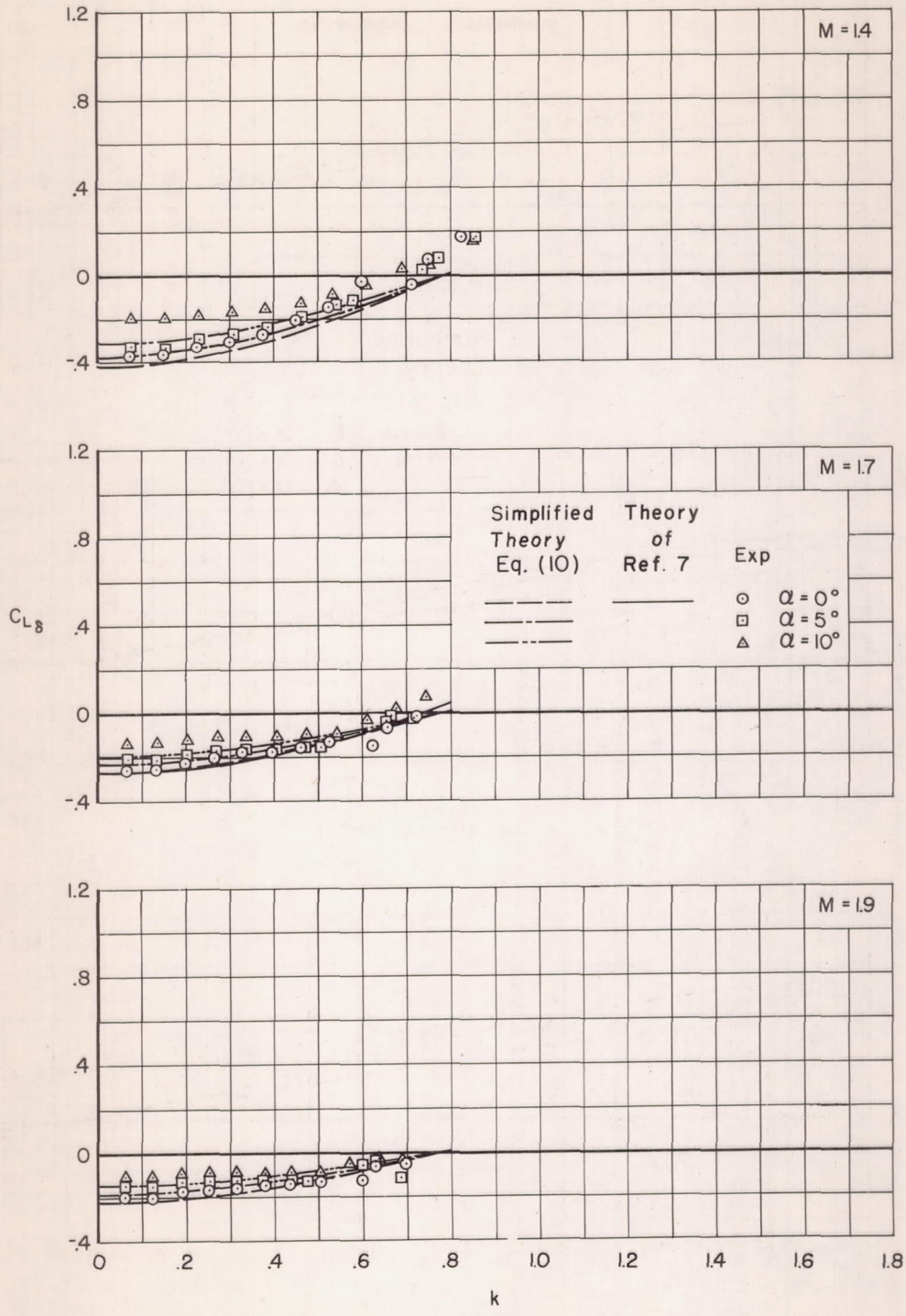


(b) Supersonic Mach numbers.

Figure 4.- Concluded.

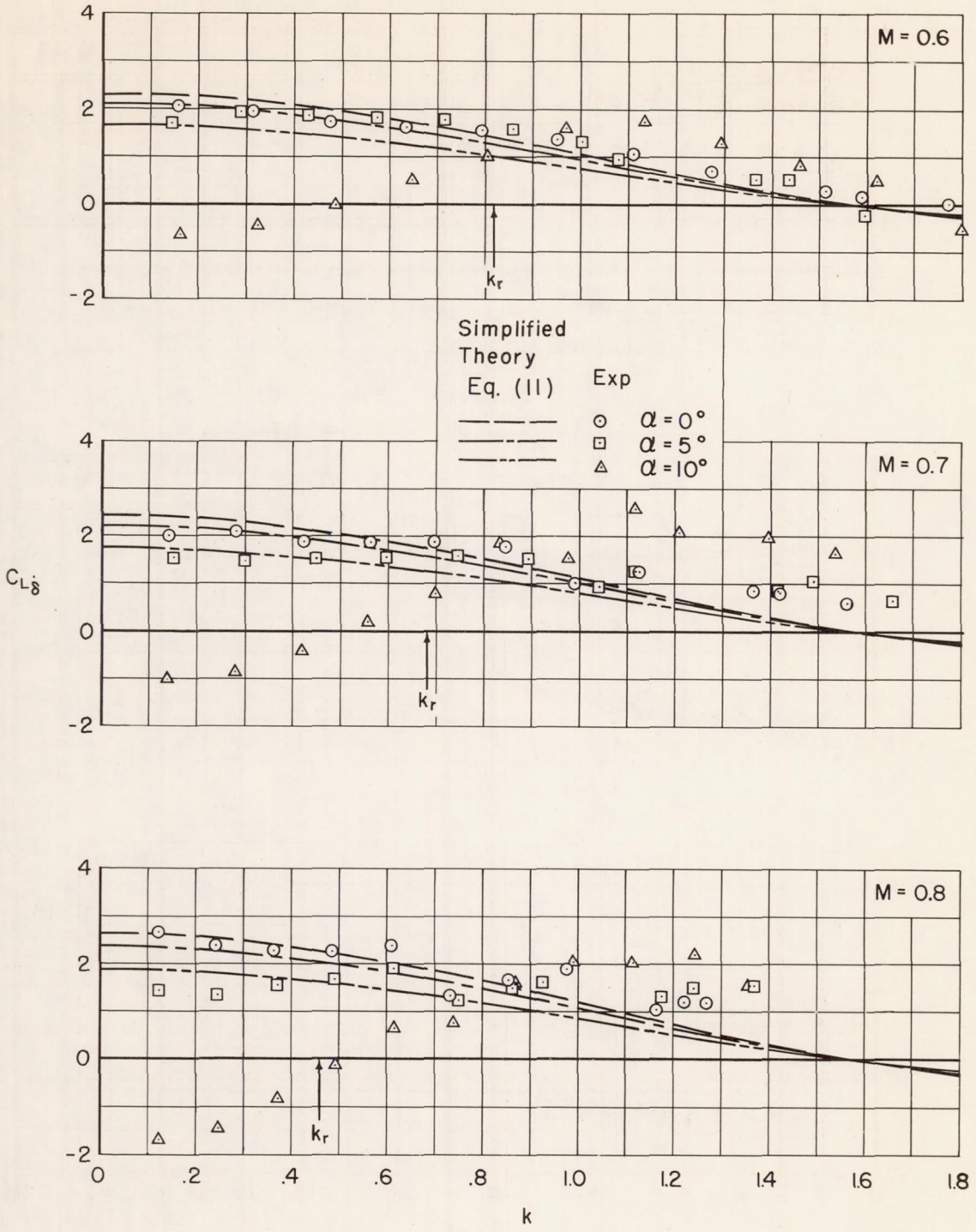


(a) Subsonic Mach numbers.

Figure 5.- Variation of out-of-phase lift derivative with reduced frequency.

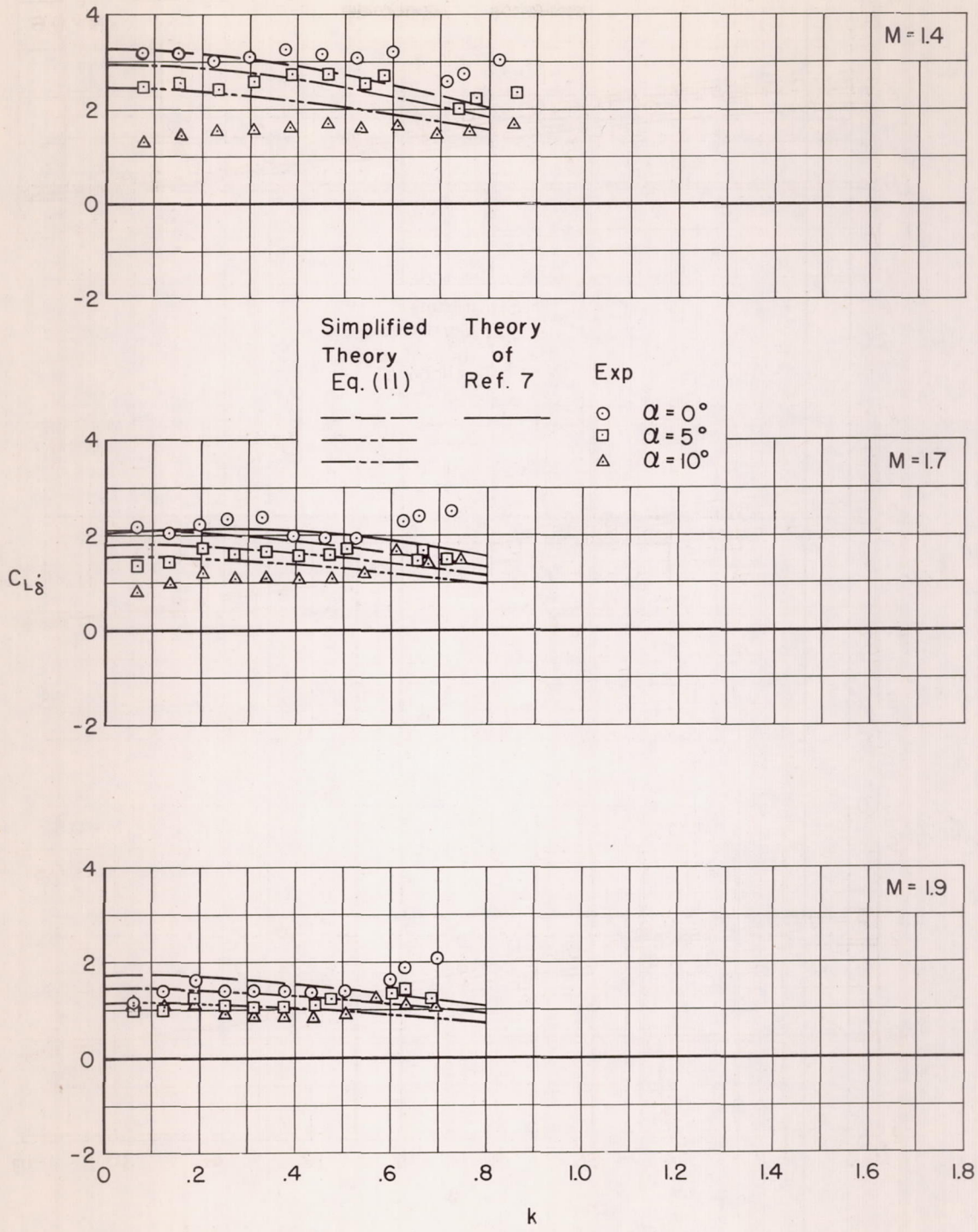


(b) Supersonic Mach numbers.

Figure 5.- Concluded.

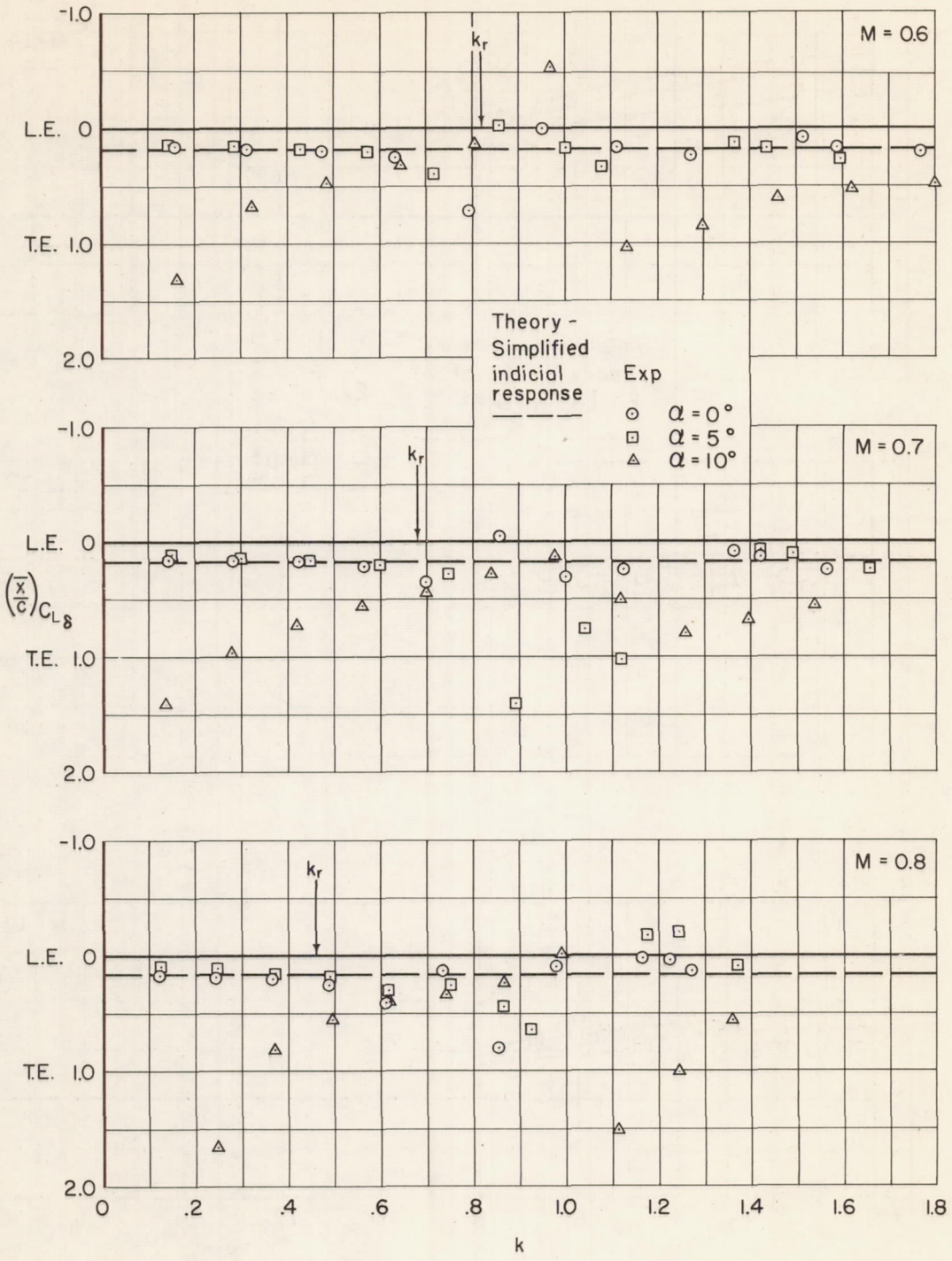


(a) Subsonic Mach numbers.

Figure 6.- Variation of center of pressure of in-phase lift with reduced frequency.

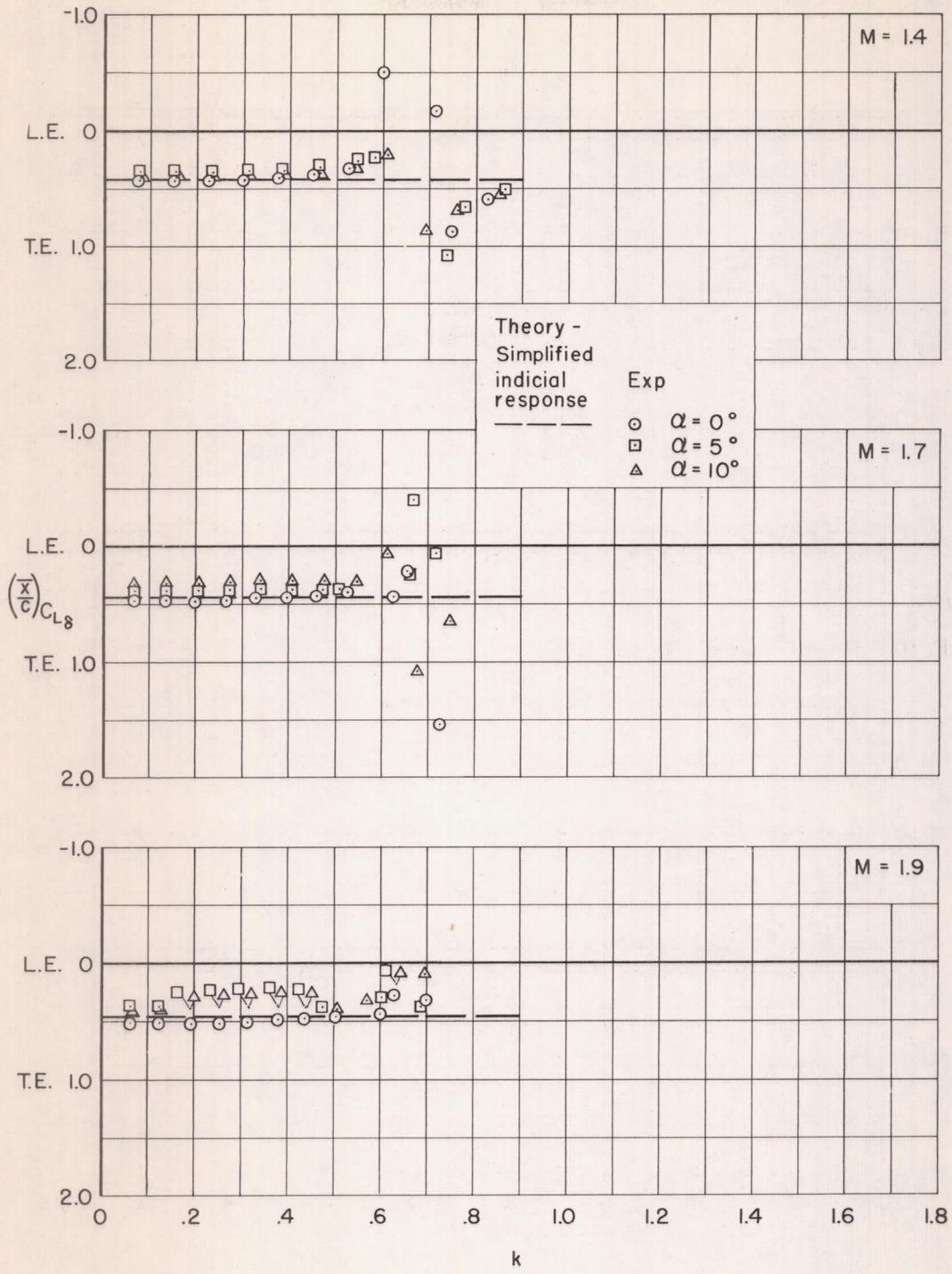


(b) Supersonic Mach numbers.

Figure 6.- Concluded.

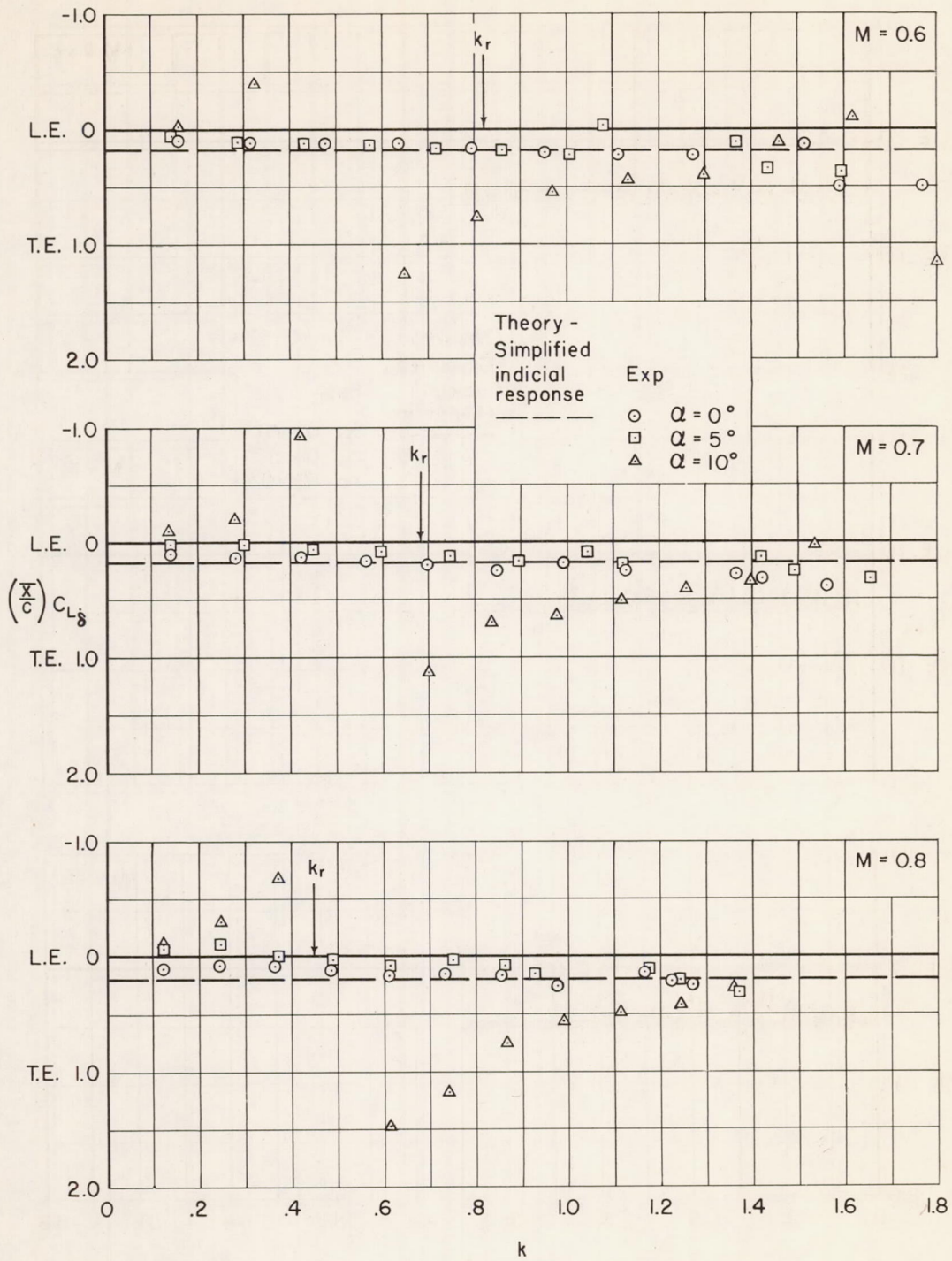


(a) Subsonic Mach numbers.

Figure 7.- Variation of center of pressure of out-of-phase lift with reduced frequency.

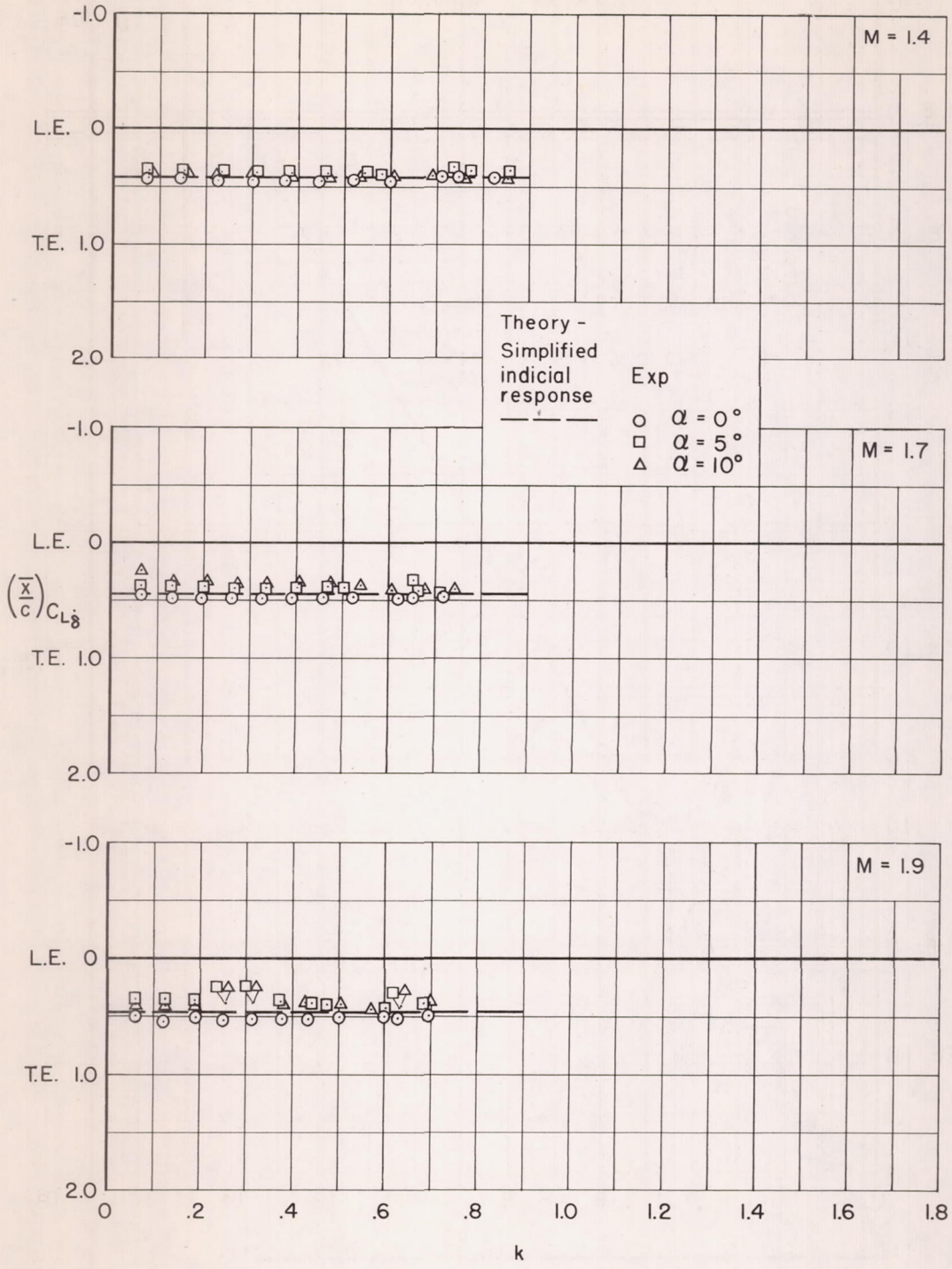


(b) Supersonic Mach numbers.

Figure 7.- Concluded.

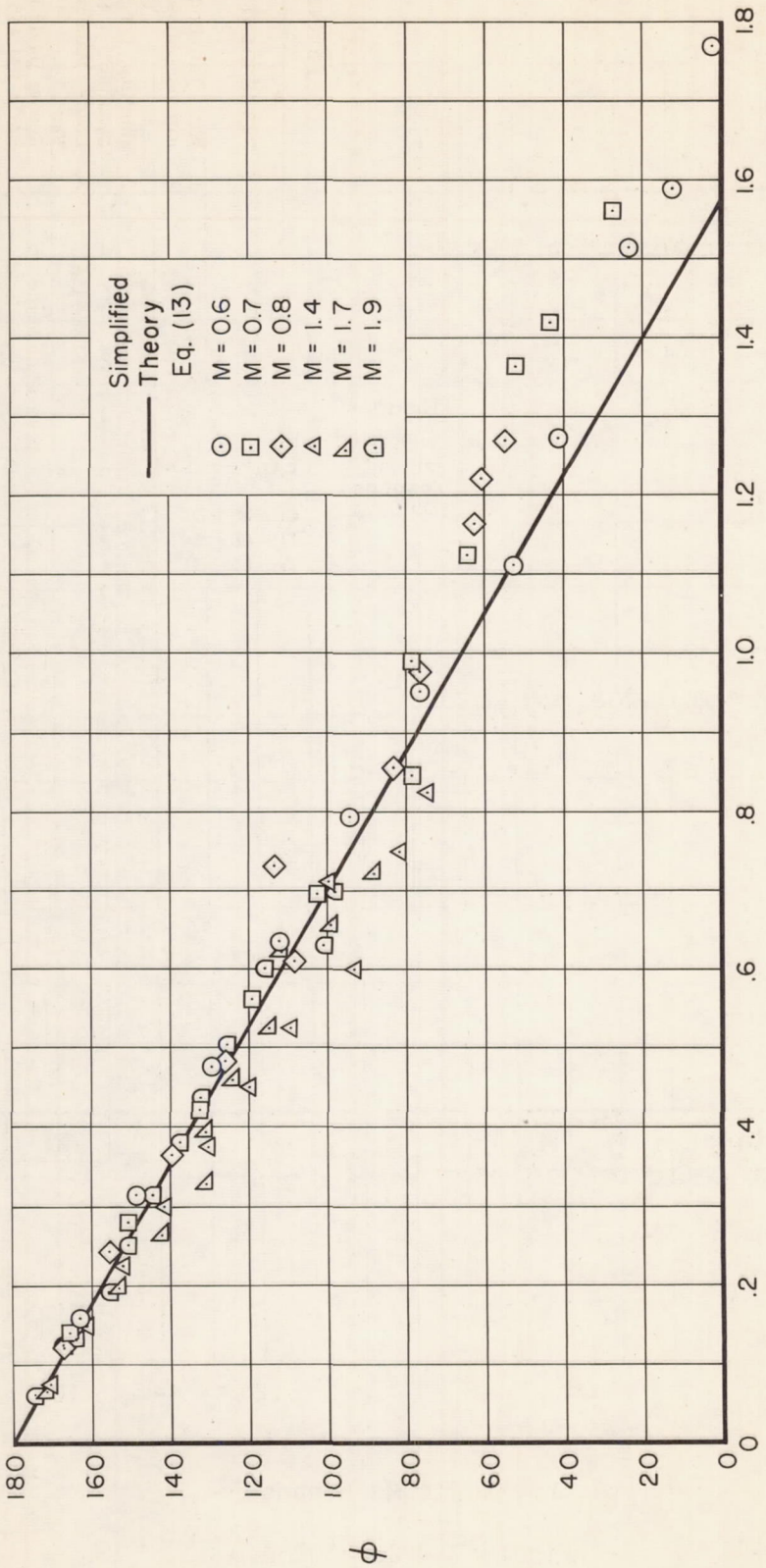


Figure 8.- Variation of phase angle with reduced frequency; $\alpha = 0^{\circ}$.



NACA - Langley Field, Va.